



Concatemers to re-investigate the role of $\alpha 5$ in $\alpha 4\beta 2$ nicotinic receptors

Marie S. Prevost¹ · Hichem Bouchenaki¹ · Nathalie Barilone¹ · Marc Gielen^{1,2} · Pierre-Jean Corringer¹

Received: 22 November 2019 / Revised: 15 May 2020 / Accepted: 22 May 2020 / Published online: 29 May 2020
© Springer Nature Switzerland AG 2020

Abstract

Nicotinic acetylcholine receptors (nAChRs) are pentameric ion channels expressed in the central nervous systems. nAChRs containing the $\alpha 4$, $\beta 2$ and $\alpha 5$ subunits are specifically involved in addictive processes, but their functional architecture is poorly understood due to the intricacy of assembly of these subunits. Here we constrained the subunit assembly by designing fully concatenated human $\alpha 4\beta 2$ and $\alpha 4\beta 2\alpha 5$ receptors and characterized their properties by two-electrodes voltage-clamp electrophysiology in *Xenopus* oocytes. We found that $\alpha 5$ -containing nAChRs are irreversibly blocked by methanethiosulfonate (MTS) reagents through a covalent reaction with a cysteine present only in $\alpha 5$. MTS-block experiments establish that the concatemers are expressed in intact form at the oocyte surface, but that reconstitution of nAChRs from loose subunits show inefficient and highly variable assembly of $\alpha 5$ with $\alpha 4$ and $\beta 2$. Mutational analysis shows that the concatemers assemble both in clockwise and anticlockwise orientations, and that $\alpha 5$ does not contribute to ACh binding from its principal (+) site. Reinvestigation of suspected $\alpha 5$ -ligands such as galantamine show no specific effect on $\alpha 5$ -containing concatemers. Analysis of the $\alpha 5$ -D398N mutation that is linked to smoking and lung cancer shows no significant effect on the electrophysiological function, suggesting that its effect might arise from alteration of other cellular processes. The concatemeric strategy provides a well-characterized platform for mechanistic analysis and screening of human $\alpha 5$ -specific ligands.

Keywords Neuropharmacology · Biochemical pharmacology · Ligand-gated ion channels · Nicotinic receptors · Concatemers

Abbreviations

| | |
|------|------------------------------|
| ACh | Acetylcholine |
| GABA | γ -Amino butyric acid |
| GFP | Green fluorescent protein |
| MTS | Methanethiosulfonate |

| | |
|-------|---|
| nAChR | Nicotinic acetylcholine receptor |
| SCAM | Substituted cysteine accessibility method |

Introduction

Nicotinic receptors form a family of acetylcholine (ACh) gated ion channels that are widely expressed in the nervous system. They result from the assembly of 5 subunits taken from a repertoire of 16 subunit genes in the human genome. In the brain, a single subunit $\alpha 7$ can form homopentamers, while the others contain both principal ($\alpha 2$, 3, 4, 6) and complementary ($\beta 2$, 4) subunits, together or not with an accessory ($\alpha 5$, $\beta 3$) subunit. The combinatorial association of various subunits thus generates a large repertoire of receptors. Genomic studies associate the $\alpha 5$ gene to smoking and lung cancer through the existence of a polymorphism that produces a protein variant of $\alpha 5$ (D398N) [1]. In mice, $\alpha 4^{-/-}$ and $\beta 2^{-/-}$ genotypes fail to self-administer nicotine, while $\alpha 5^{-/-}$ genotype displays a unique altered behavior towards nicotine, with partly reduced nicotine-related

Marie S. Prevost and Hichem Bouchenaki contributed equally to the work.

Electronic supplementary material The online version of this article (<https://doi.org/10.1007/s00018-020-03558-z>) contains supplementary material, which is available to authorized users.

- ✉ Marc Gielen
marc.gielen@pasteur.fr
- ✉ Pierre-Jean Corringer
pierre-jean.corringer@pasteur.fr

¹ Unité Récepteurs-Canaux, Institut Pasteur, UMR 3571, CNRS, 75015 Paris, France

² Sorbonne Université, 21, rue de l'école de médecine, 75006 Paris, France

behaviors [2–4] and also towards ethanol, whose effects are partly enhanced [5], together with anxiety-related behaviors [6]. In rats, a recent study also highlighted a phenotype linked to nicotine and alcohol relapse processes [7, 8]. In the brain, $\alpha 5$ incorporates in $\alpha 3\beta 4\alpha 5$ and $\alpha 4\beta 2\alpha 5$ nAChRs, and both nAChRs may contribute to these effects. Among them, $\alpha 4\beta 2\alpha 5$ nAChRs in the dorsal striatum were found critical to regulate dopamine transmission and release [1, 9, 10]. Likewise, deletion of $\alpha 5$ in ventral tegmental dopaminergic neurons, which also express $\alpha 4$ and $\beta 2$, markedly shifts to higher concentrations nicotine-elicited increase in neuron firing as well as nicotine self-administration. These effects are reversed, either totally or partially, by the re-expression of wild-type *versus* D398N $\alpha 5$ subunit [3, 11]. These observations indicate a key contribution of the $\alpha 4\beta 2\alpha 5$ combination in addictive processes.

Despite their therapeutic potential in physiology and translation, $\alpha 4\beta 2\alpha 5$ nAChRs are poorly understood. This is due to the intricate assembly of the subunits that associate in various stoichiometries. First, co-expression in recombinant systems of $\alpha 4$ and $\beta 2$ generates two populations of functional receptors: $1/(\alpha 4)_2(\beta 2)_3$, carrying two ACh binding sites at the interface between the “principal” or (+) face of $\alpha 4$ and the “complementary” or (–) face of $\beta 2$ [named $\alpha 4(+)-\beta 2(-)$ sites], and $2/(\alpha 4)_3(\beta 2)_2$, carrying two $\alpha 4(+)-\beta 2(-)$ sites and one $\alpha 4(+)-\alpha 4(-)$ site, this latter displaying low ACh affinity [12]. Additional co-expression of the $\alpha 5$ subunit is thought to mostly yield a receptor with a $(\alpha 4)_2(\beta 2)_2\alpha 5$ stoichiometry, with unknown number of ACh binding sites since it is not clear whether $\alpha 5$ can participate to one, and since $\alpha 5$ can potentially occupy any position within the pentamer.

Detailed functional and pharmacological study of these receptors requires overcoming the “stoichiometry issue”. Two main strategies have been developed: (1) by varying with the ratios of transfected/injected DNAs of the distinct subunits, which is assumed to favor the proportion of a particular subunit in the pentamer, but this technique cannot certify that a single stoichiometry is being expressed; (2) another approach is to fuse the subunits into concatemeric nAChRs whose subunits are covalently connected by linkers of various sizes. However, di-, tri-, tetramers were found not to definitely solve the stoichiometry issue [13], and the current approach is to generate fully concatenated pentameric receptors that are thought to unambiguously constrain the stoichiometry, providing that the protein is not cleaved within the cell.

Several pentameric concatemers of heteromeric receptors have been described incorporating the $\alpha 4\beta 2$ and $\alpha 3\beta 4$ subunits [11, 14–22], as well as the $\alpha 3\beta 4\alpha 5$ subunits [11, 19]. In contrast, a single study described the $\alpha 4\beta 2\alpha 5$ combination, with an arrangement ($\beta 2\alpha 4\alpha 5\alpha 4\alpha 4/\beta 2$) where only one $\alpha 4\beta 2$ pair (and therefore one canonical $\alpha 4/\beta 2$ binding site) is present in the pentamer and that are endowed with weak

ACh-gated currents (less than 50 nA in oocytes [19]). In the present paper, we describe $\alpha 4\beta 2\alpha 5$ containing concatemers where $\alpha 5$ is assembled with two $\alpha 4\beta 2$ pairs and that generate substantial (in the 0.1–1 μ A range) ACh-gated currents. This enables unambiguous expression of defined nAChRs stoichiometries, allowing us to revisit the functional and pharmacological properties of these key receptors involved in addiction.

Methods

Molecular biology

The design of nAChR concatemers used in this study followed the same strategy as a previous concatemer design for GABA_A receptors [23]. Human $\alpha 4$, $\beta 2$ and $\alpha 5$ nAChR subunits were first subcloned into the pRK5 vector. To enhance expression in *Xenopus* oocytes, a 37 bp 5'UTR region of *Xenopus* β -globin mRNA was added upstream of the open reading frame in pRK5 and the Kozak sequence was optimized. To facilitate the cloning, the endogenous HindIII and NheI sites from the $\beta 2$ subunit were removed by site directed mutagenesis.

Inverse PCR was further used to add 20 primer-encoded glutamines to the C-terminal end of the $\alpha 4$ subunits and 15 to the end of the $\alpha 5$ and $\beta 2$ subunits—except for subunits used as the last subunit in the concatemers—and the individual subunits were cloned to be flanked by unique restriction sites.

The five subunits were then assembled into a single open reading frame between ClaI and HindIII sites, with the first subunit containing a signal peptide ($\alpha 4$ signal peptide for the $3(\alpha 4)$, $3(\beta 2)$ and $\alpha 5_{\text{last}}$ concatemers; $\alpha 5$ signal peptide for the $\alpha 5_{\text{first}}$ concatemer). All the other subunits were composed only of their mature proteins as described in the Uniprot.

The final arrangements are: for the $3(\alpha 4)$ concatemer ClaI-Kozak-SP($\alpha 4$)- $\alpha 4$ -Q20-AgeI- $\beta 2$ -15Q-SalI- $\alpha 4$ -20Q-NheI- $\beta 2$ -15Q-XhoI- $\alpha 4$ -Stop-HindIII, for the $3(\beta 2)$ concatemer ClaI-Kozak-SP($\alpha 4$)- $\alpha 4$ -20Q-AgeI- $\beta 2$ -15Q-SalI- $\alpha 4$ -20Q-NheI- $\beta 2$ -15Q-XhoI- $\beta 2$ -Stop-HindIII, for the $\alpha 5_{\text{last}}$ concatemer ClaI-Kozak-SP($\alpha 4$)- $\alpha 4$ -20Q-AgeI- $\beta 2$ -15Q-SalI- $\alpha 4$ -20Q-NheI- $\beta 2$ -15Q-XhoI- $\alpha 5$ -Stop-HindIII and for the $\alpha 5_{\text{first}}$ concatemer ClaI-Kozak-SP($\alpha 5$)- $\alpha 5$ -15Q-AgeI- $\beta 2$ -15Q-SalI- $\alpha 4$ -20Q-NheI- $\beta 2$ -15Q-XhoI- $\alpha 4$ -Stop-HindIII.

Concatemers containing selected point mutations in particular subunits were constructed by mutating the corresponding single subunits, which were then cloned back into the concatemer.

When specified, we used GFP-fusion concatemers, inspired from Nashmi et al. [24]: the coding sequence of the eGFP was inserted in the intracellular domain of $\alpha 4$

between Lys423 and Ser424 (according to the Uniprot P43681 numbering) to give the following arrangement [... PGPSCK-eGFP-SPSDQL...].

HEK cells expression and Western blotting

HEK293 cells were cultured in 100 mm dishes in DMEM containing fetal bovine serum (10% v/v) and antibiotics (penicillin/streptomycin, 10 U/ml and 10 μ g/ml respectively), and 10 μ g DNA was transfected using JetPrime reagent (Polyplus) according to manufacturer instructions. After 48 h expression at 37 °C, cells were resuspended in lysis buffer containing 150 mM Tris pH 7.6, 200 mM NaCl and 1% Triton, and used for Western blotting. Western blotting was performed using mouse anti-GFP antibody (Invitrogen) and goat anti-mouse HRP-coupled antibody (Vectorlabs), and revealed with SuperSignal West Pico ECL kit (ThermoPierce).

Two-electrode voltage-clamp electrophysiology

Xenopus laevis oocytes were obtained from Centre de Ressources Biologiques-Rennes, France or from EcoCyte Bioscience, Germany, and maintained in modified Barth's medium (88 mM NaCl, 1 mM KCl, 1 mM MgSO₄, 2.5 mM NaHCO₃, 0.7 mM CaCl₂, 5 mM HEPES pH 7.3). Defolliculated oocytes were submitted to intranucleus injection of 2–5 ng of cDNA and kept at 18 °C for 2–5 days before recording.

For DNA ratio injections, cDNA sequences of human $\alpha 4$, $\beta 2$ and $\alpha 5$ inserted in pRK5 vectors were mixed to the desired ratio while keeping a constant total DNA concentration of 0.06 ng/nl, and were recorded 1–2 days after injection.

Recordings were performed with a Digidata 1550A (Molecular Devices) digitizer, an Oocyte Clamp OC-725C (Warner Instruments) amplifier and using the pClamp 10.5 software. Oocytes were perfused with Ringer's buffer (100 mM NaCl, 2.5 mM KCl, 2 mM CaCl₂, 1 mM MgCl₂, 10 mM HEPES pH 7.3) using a gravity-driven system. Drugs were applied after dilution in Ringer's buffer. MTSEA solutions were prepared immediately before recording. All currents were measured at –60 or –80 mV.

Data analysis

Recordings were analyzed using ClampFit, AxoGraph X, Plot and GraphPad Prism. Measurements were performed at the peak of the response. Except when stated otherwise, for concentrations response curves, points were fitted to a mono- or bi-phasic Hill equation for each cell before averaging EC₅₀ and Hill slopes. For the statistical comparisons using GraphPad Prism, we performed Student's *t* tests when

comparing two groups and one-way ANOVA when comparing more than two groups (with Dunnett's or Tukey's post hoc tests, depending on whether the data are compared to a control group or not). Figures representing published X-ray structures were prepared using PyMol. Figures were prepared using GraphPad Prism and Inkscape.

Results

Concatemer design and characterization

Concatemer design

The design we adopted is “Signal Peptide (SP)– α – β – α – β – α/β ”, giving for the $\alpha 4\beta 2$ constructs SP_($\alpha 4$)– $\alpha 4$ – $\beta 2$ – $\alpha 4$ – $\beta 2$ – $\alpha 4$, called the 3($\alpha 4$) concatemer, and SP_($\alpha 4$)– $\alpha 4$ – $\beta 2$ – $\alpha 4$ – $\beta 2$ – $\beta 2$, called the 3($\beta 2$) concatemer (Fig. 1a). For $\alpha 4\beta 2\alpha 5$ concatemers, we generated two constructs, one where $\alpha 5$ and its SP are inserted as the first subunit, SP_($\alpha 5$)– $\alpha 5$ – $\beta 2$ – $\alpha 4$ – $\beta 2$ – $\alpha 4$, called the $\alpha 5_{\text{first}}$ concatemer, and another construct where $\alpha 5$ is inserted as a last subunit, SP_($\alpha 4$)– $\alpha 4$ – $\beta 2$ – $\alpha 4$ – $\beta 2$ – $\alpha 5$, called $\alpha 5_{\text{last}}$. We chose the linkers based on sequences alignment and the $\alpha 4\beta 2$ X-ray structures [25]. It consists of 15 or 20 glutamine residues plus 2 residues corresponding to unique restriction sites used for cloning (Thr-Gly, Val-Asp, Ala-Ser and Leu-Glu in this order), a strategy already used to generate pentameric GABA_A concatemers [23]. To compensate the fact that, as compared to $\alpha 5$ and $\beta 2$, the C-terminus of $\alpha 4$ (post-M4 helix) is shorter by 12 and 15 residues respectively, the linkers are 15 glutamines long in the $\alpha 4$ – $\beta 2$ connection and 20 glutamines long for the $\alpha 5$ – $\beta 2$, $\beta 2$ – $\alpha 4$ and $\beta 2$ – $\alpha 5$ ones.

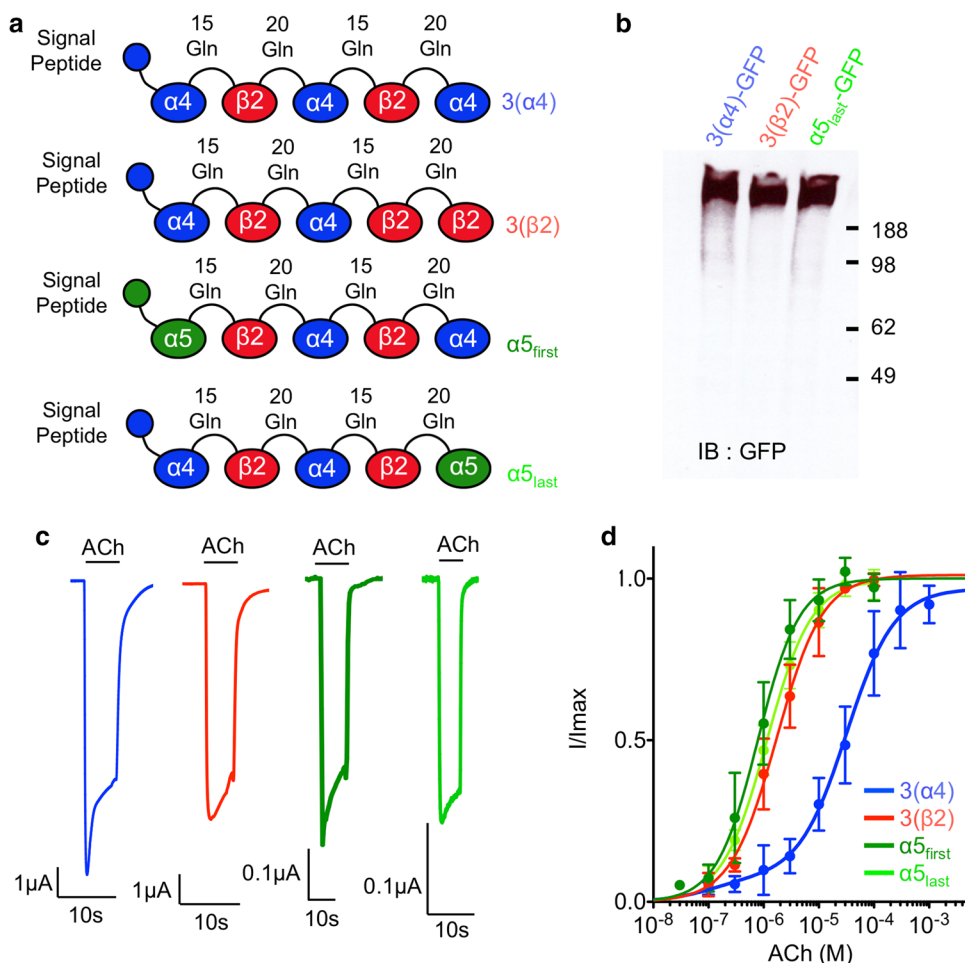
Concatemers metabolic stability

To assess the metabolic stability of the concatemers, we selected a representative subset of constructs. We inserted the GFP coding sequence in the 3($\alpha 4$), 3($\beta 2$) and $\alpha 5_{\text{last}}$ concatemers. GFP was inserted within the intracellular domain of $\alpha 4$ similarly to previous work on the mouse $\alpha 4$ [24], and in the first subunit of the concatemer to visualize all sub-products if any. Constructs were transfected in HEK cells and whole cell extracts were subjected to Western blot analysis against GFP. All constructs show a single band at a high molecular weight >190 kDa, consistent with a pentameric concatemer, showing that the protein undergoes little, if any, degradation (Fig. 1b).

Concatemers ACh concentration–response curves

Concatemers were expressed in *Xenopus* oocytes and acetylcholine-evoked currents were recorded by two-electrode

Fig. 1 A robust concatemer design. **a** Schematic of the concatemers' arrangement. Each subunit is depicted by an oval, with the first subunit in the N-terminal having its signal peptide as a circle. Linkers are depicted with a black line. **b** Anti-GFP Western blotting of whole extracts of HEK cells expressing the designated concatemer. **c** Sample traces recorded on oocytes expressing the 3($\alpha 4$) (blue), 3($\beta 2$) (red), $\alpha 5_{\text{first}}$ (dark green) and $\alpha 5_{\text{last}}$ (light green) concatemers. For the 3($\alpha 4$), ACh concentration was 100 μM , and for the 3($\beta 2$) and the $\alpha 5$, ACh concentration was 10 μM . **d** ACh concentration–response curves of the currents recorded for the four concatemers. Points are mean \pm SD, with $n \geq 7$



voltage-clamp electrophysiology. The 3($\alpha 4$) and 3($\beta 2$) concatemers generate robust currents in the 1–10 μA range, while $\alpha 5$ concatemers generate lower, yet reasonable, currents in the 0.1–1 μA range, with some cells displaying maximal currents above 1 μA (Fig. 1c). ACh concentration–response curve of the 3($\beta 2$) and the $\alpha 5$ concatemers are similar with EC_{50} s of 1.45, 0.75 and 1.17 μM for 3($\beta 2$), $\alpha 5_{\text{first}}$ and $\alpha 5_{\text{last}}$ respectively (Fig. 1d, Supplementary Table 1). The 3($\alpha 4$) concatemer, known to carry an additional low affinity $\alpha 4$ – $\alpha 4$ site, yields a biphasic curve as expected. Constraining the high-affinity EC_{50} to 1 μM yields a second component with an EC_{50} of 28.9 μM . All values are consistent with the literature on $\alpha 4\beta 2$ receptors, both on loose subunits [17, 26] and on pentameric concatemeric $\alpha 4\beta 2$ constructs [17].

Rotational direction of concatemers

In 2018, Ahring and colleagues showed that concatemers of nicotinic receptors often assemble readily in both the clockwise and the counterclockwise orientations, yielding heterogeneity of subunit arrangements within the pentamer even for fully concatenated constructs (Supplementary Fig. 1).

Their approach was based on the use of the positive modulator NS9283 [13]. NS9283 was shown by X-ray crystallography to occupy the orthosteric site of the acetylcholine binding protein [27]. On the $\alpha 4\beta 2$ nAChR, NS9283 potentiation is disrupted by three-point mutations introducing a VFL $\beta 2$ -specific motif on the complementary face of the $\alpha 4$ subunit [13] (Supplementary Fig. 2), while introducing the HQT $\alpha 4$ -specific motif on the complementary face of the $\beta 2$ subunit converts it into an agonist. Combined data strongly support that NS9283 binds specifically at the $\alpha 4$ – $\alpha 4$ interface [27]. Single channel measurements also showed that NS9283 potentiation was sensitive to mutations performed on the principal face of the $\beta 2$ subunit [22].

Considering the 3($\alpha 4$) concatemer, a clockwise orientation would place the first $\alpha 4$ subunit contributing to the (–) face of the $\alpha 4$ – $\alpha 4$ site, and conversely an anticlockwise orientation would place the 5th subunit in this position. NS9283 binding specifically at the $\alpha 4$ – $\alpha 4$ interface, a fixed orientation of the concatemer should thus yield an alteration of its binding when mutating only one of the two terminal subunits (Fig. 2a). We thus introduced the mutation triplets in the $\alpha 4$ subunits of the 3($\alpha 4$) concatemer,

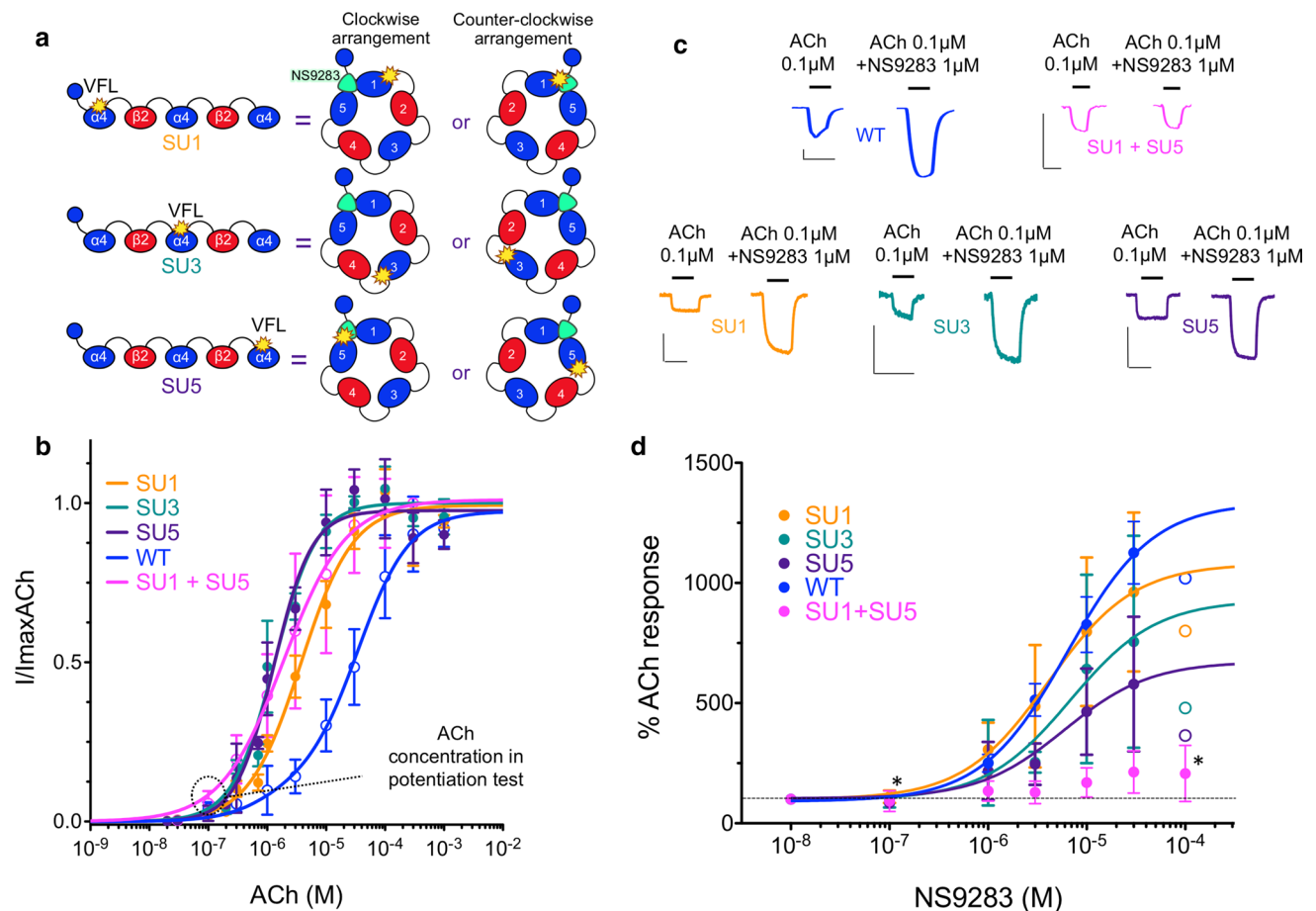


Fig. 2 Rotation direction of the 3($\alpha 4$) concatemer. **a** Potential integrity of the NS9283 binding site depending on the position of the VFL triple-mutation. In the WT, NS9283 binds at the $\alpha 4$ – $\alpha 4$ interface. In the triple-mutation VFL situation on all three $\alpha 4$ subunits, the NS9283 binding site is impaired and no potentiation is detected (Ahring 2017). When the VFL mutation is introduced in the middle $\alpha 4$ subunit (“SU3”) the NS9283 binding site is predicted to be intact. When it is introduced in the first (“SU1”) or the last (“SU5”) $\alpha 4$ subunit, pentamers that adopt an orientation that makes the VFL residues pointing in the NS9283 binding site should not be potentiated anymore. **b** ACh concentration–response curves of WT, SU1, SU3, SU5 and SU1 + SU5 constructs show that all mutants display gain-of-function phenotypes towards ACh, as previously described (Ahring

2017). Points are mean \pm SD, with $n \geq 3$. Unlike the original study, we choose a test ACh concentration that would allow to observe clear potentiation for the 3 constructs: 0.1 μ M which is around the EC_{10} of SU3, SU5 and SU1 + SU5, and EC_{05} of SU1. **c** Example traces of NS9283 potentiation of the WT and the VFL mutants. Vertical bar is 100 nA, horizontal bar is 10 s. **d** Concentration–response curves of the potentiation of 0.1 μ M ACh currents by NS9283. A dash line is drawn to figure 100%. Values measured for 100 μ M NS9283 were not included in the curve fit because they were reproducibly lower than the 30 μ M values, possibly due to a channel block effect, but they are still displayed as empty circles. Points are mean \pm SD with $n \geq 3$. * for SU1 + SU5, a Student’s *t* test found those two values to be non-statistically different

one subunit at a time (calling the resulting constructs SU1, SU3 and SU5). We also constructed a concatemer in which both the 1st and the 5th subunit harbor the VFL triplet (SU1 + SU5). ACh concentration response shows marked gain of function effect of the mutations on the four constructs (Fig. 2b and Supplementary Table 1), showing an increase of the ACh apparent affinity as compared to the WT. Thus, to reliably evaluate the potentiation by NS9283, we used an ACh test concentration of 0.1 μ M which is below the EC_{20} of the four constructs. On the WT 3($\alpha 4$) concatemer, when we co-applied ACh at 0.1 μ M

with 0.1, 1, 3, 10, 30 and 100 μ M of NS9283, we observed a dose-dependent potentiation of the currents as previously described (Fig. 2c, d). We controlled that NS9283 does not significantly potentiate the ACh-gated currents of the SU1 + SU5 construct, in agreement with its binding at the $\alpha 4$ – $\alpha 4$ interface [13] (Fig. 2c, d). Strikingly, all single-subunit mutations, SU1, SU3 and SU5 constructs, display robust potentiation of the currents by NS9283 (Fig. 2c, d). We conclude that the 3($\alpha 4$) concatemer produces a mixture of both orientations at the cell surface (Fig. 2a), both participating substantially to the electrophysiological response.

Investigating $\alpha 5$ -nAChR pharmacology

For the sake of simplicity, and if not stated otherwise, we show here data related to the $\alpha 5_{\text{first}}$ concatemer, first because it displays similar properties to those of the $\alpha 5_{\text{last}}$, and second because, as shown above, the mixture of orientations likely results in the same mixture of orientations for both constructs (Supplementary Fig. 1). In the search for $\alpha 5$ ligands, we investigated compounds that were described in the literature to bind to the $\alpha 5$ subunit from work on loose or partially concatenated subunits.

ACh and Sazetidine-A

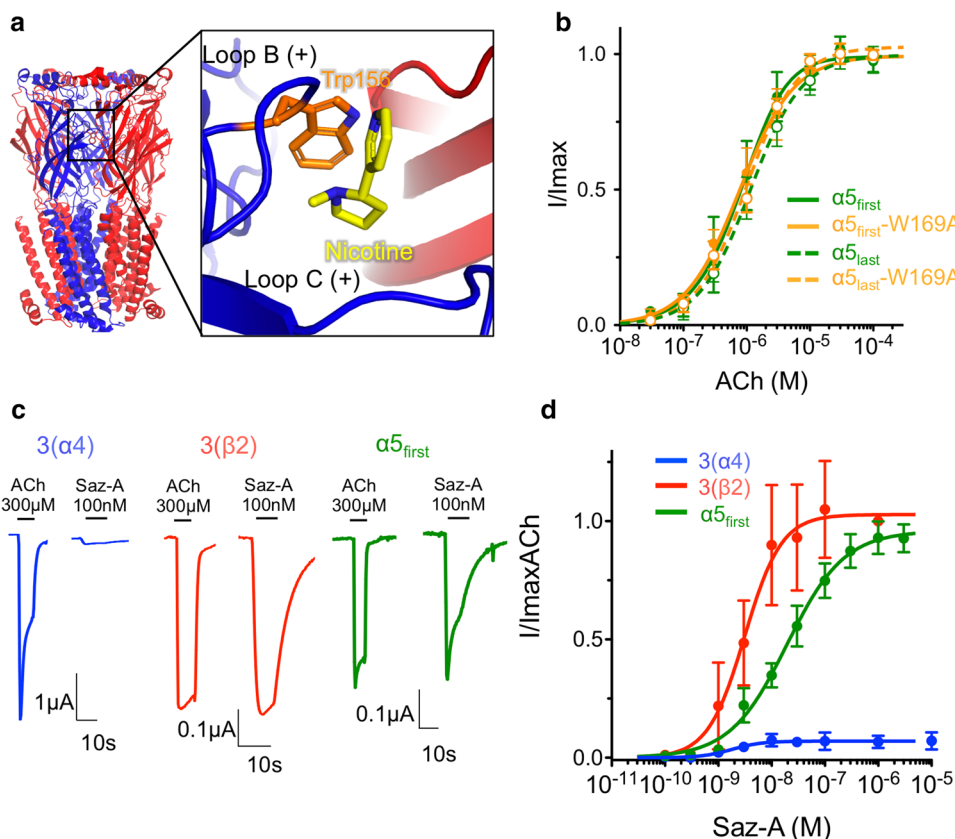
Since co-expression of $\alpha 5$ and $\beta 2$ without $\alpha 4$ does not generate functional channels, it is believed that $\alpha 5$ does not contribute to the principal component of the ACh site, but this idea has been challenged in a recent study [28]. In $\alpha 4\beta 2$ nAChRs, the canonical ACh binding site is well characterized, as illustrated by the X-ray structures of $\alpha 4_2\beta 2_3$ in complex with nicotine [25] (Fig. 3a). The site is composed of three regions called loops from the principal $\alpha 4$ component, each of them contributing aromatic residues to bind the positive ammonium moiety of the ligand, and four regions of the complementary $\beta 2$ component. The principal component is only partially conserved in $\alpha 5$, questioning its ability to

bind ACh from of its (+) face (Supplementary Figs. 1 and 2). For instance, some critical aromatic residues in the (+) face of $\alpha 4$ are present in $\alpha 5$ (Trp in Loop B, the key binding aromatic residue stabilizing the ligand through cation-pi interaction [29], as well as Tyr C2), while some are absent (Tyr in Loop A and Loop C1).

If $\alpha 5(+)$ contributes to ACh binding, its mutation should alter the ACh EC_{50} as recorded by TEVC. To challenge this idea, we mutated the $\alpha 5$ Loop B Trp in $\alpha 5_{\text{first}}$ and in $\alpha 5_{\text{last}}$ into alanine ($\alpha 5$ -W169A). Concentration–response curves of the $\alpha 5$ -W169A concatemers are indistinguishable from the WT with EC_{50} of 0.87 and 1.00 μM respectively, and nH of 1.00 and 1.08 (Fig. 3b, Supplementary Table 1). This suggests that the (+) face of $\alpha 5$ does not bind ACh. This idea is fully consistent with our observation that the $\alpha 5$ and the $3(\beta 2)$ concatemers (which carry an $\alpha 5$ or a $\beta 2$ subunit at the “accessory” position) have highly similar EC_{50} for ACh.

However, in the course of our pharmacological investigations, we observed that the $\alpha 5_{\text{first}}$ and the $3(\beta 2)$ concatemers have different concentration–response curves for sazetidine. Sazetidine-A (Saz-A) is a full agonist of $\alpha 4_2\beta 2_3$ nAChRs but a partial agonist of $\alpha 3\beta 2$ since it does not bind to the $\alpha 4$ – $\alpha 4$ interface [30, 31]. On the $3(\alpha 4)$ concatemers, Saz-A generates small currents that do not exceed $6.0 \pm 2\%$ of the maximal response to ACh (Fig. 3c and Supplementary Table 1). In contrast, we found that Saz-A is a full agonist on both

Fig. 3 The orthosteric site. **a** The nicotine binding pocket in the $\alpha 4\beta 2$ X-ray structure visualized using PyMol (Morales-Perez 2018, pdb 5KXI). $\alpha 4$ subunit is shown in blue cartoon representation, $\beta 2$ in red cartoon representation. Loop B and Loop C are labeled, Trp 156 is shown in orange stick representation and nicotine is depicted in yellow stick representation. **b** ACh concentration–response curves for the $\alpha 5$ concatemers WT and W169A mutant. Points are mean \pm SD with $n \geq 3$. **c** Sample traces of the effect of saturating concentrations of ACh and Sazetidine-A (Saz-A) on a single oocyte for the three concatemers. **d** Concentration–response curves for Saz-A of the three concatemers. Currents were normalized with the maximal current recorded with ACh for each cell. Points are mean \pm SD with $n \geq 6$



$\alpha 5_{\text{first}}$ and $3(\beta 2)$ concatemers, but it displays higher EC_{50} and lower cooperativity for $\alpha 5_{\text{first}}$ (22 nM and $nH=0.86$ as compared to $3(\beta 2)$ 6.6 nM and $nH=1.58$, Fig. 3d and Supplementary Table 1). Interestingly, looking at the concatemer assemblies in both rotational directions allows proposing a simple interpretation of this discrepancy. While the clockwise and anticlockwise assemblies of the $3(\beta 2)$ concatemer both carry two $\alpha 4(+)-\beta 2(-)$ sites, the clockwise assembly of $\alpha 5_{\text{first}}$ carries two $\alpha 4(+)-\beta 2(-)$ sites but the anticlockwise assembly of $\alpha 5_{\text{first}}$ carries one $\alpha 4(+)-\beta 2(-)$ site and one $\alpha 4(+)-\alpha 5(-)$ site. The lower cooperativity of $\alpha 5_{\text{first}}$ suggests the contribution of a heterogeneous class of binding sites, and we infer that, in the anticlockwise assembly, the $\alpha 4(+)-\alpha 5(-)$ site might display an affinity similar to that of the $\alpha 4(+)-\beta 2(-)$ for ACh, but a lower affinity for sazetidine.

A lower affinity of sazetidine for the $\alpha 4(+)-\alpha 5(-)$ site would also be in line with its stronger sensitivity toward the amino-acid composition of the complementary component of the site, which explains its inactivity on the $\alpha 4(+)-\alpha 4(-)$ site. An illustration of this are the binding modes of Sazetidine-A derivatives on ACh binding proteins (AChBP) that shows that while the ammonium moiety interacts with the aromatic box of the principal component, the rest of the compound lies on the complementary component and contacts more residues than smaller agonists, notably one hydrophobic residue from Loop E aligning with $\alpha 5\text{-Thr139}$ (Supplementary Fig. 2b, d).

Overall, our data support the idea that the $\alpha 5(+)$ face does not contribute to ACh activation in the concatemers, but they indirectly suggest that the $\alpha 4(+)-\alpha 5(-)$ interface might also bind and be activated by ACh and sazetidine, displaying respectively similar and lower affinity than the canonical $\alpha 4(+)-\beta 2(-)$ site.

Investigating other $\alpha 5$ -ligand candidates

Galantamine is an inhibitor of acetylcholine esterase and is used for treatment for Alzheimer's disease with debated efficacy. It was shown to potentiate ACh responses of the neuronal $\alpha 4\beta 2$ and $\alpha 7$ receptors by no more than 2-folds [32]. It was further described as potentiating only $\alpha 4\beta 2\alpha 5$ receptors as opposed to $\alpha 4\beta 2$ and $\alpha 4\beta 2\beta 3$ assemblies in calcium flux measurements of $\alpha 4\beta 2$ stable cell lines transfected with $\alpha 5$ [33]. More recently, another study using loose subunits surprisingly described the absence of potentiation on both $\alpha 4\beta 2$ and $\alpha 7$ receptors [34], spreading confusion on the validity of galantamine effect. Herein, we applied galantamine for 3 s or for 20 s before ACh pulses at its EC_{20} , as well as in co-application. We could not observe any significant potentiation, nor inhibition, of any of the concatemers by galantamine (Fig. 4a, b), neither $\alpha 5_{\text{first}}$ nor $3(\beta 2)$ or $3(\alpha 4)$.

Finally, we tested the neurosteroid progesterone because (1) its action on neuronal nAChRs was not investigated

further than in the original study [35], and (2) it was linked to $\alpha 5$ -nAChR modulation in $\alpha 5^{-/-}$ mice. Progesterone is soluble at 1 mg/ml in ethanol, we thus systematically applied a control solution with the ethanol concentration used in the progesterone solution. We found that 3.14 μM progesterone inhibits ACh-evoked currents on the three concatemers to similar extents (Fig. 4c, d). Thus, we conclude that progesterone is a non-selective inhibitor of $\alpha 4_3\beta 2_2$, $\alpha 4_2\beta 2_3$ and $\alpha 4_2\beta 2_2\alpha 5$ nAChRs, having similar potencies for the various assemblies.

Exploring the D398N $\alpha 5$ mutation

The $\alpha 5$ D398N single nucleotide polymorphism (SNP) was linked to nicotine addiction and lung cancer by genome-wide association studies in humans [1]. The mutation lies in the ICD, far away from the ACh/nicotine binding sites, the channel lumen or from any known allosteric modulators' sites. However, several studies have proposed various effects of the D398N on the function of recombinant $\alpha 4\beta 2\alpha 5$ and $\alpha 3\beta 4\alpha 5$ nAChRs, pointing at desensitization [36], calcium permeability [36, 37], orthosteric ligands apparent affinities [37] or maximal currents [11], effects that are rather moderate and not consistent from study to study, while one study found no effect [38].

We thus introduced the D398N mutation in the $\alpha 5$ concatemers. We first compared the metabolic stability of the WT and D398N $\alpha 5_{\text{last}}$ constructs in HEK cells, by Western blotting after insertion of GFP in the first subunit. As with the WT, we did not observe degradation of the concatemer after expression (Fig. 5a). We then injected WT and D398N $\alpha 5_{\text{first}}$ concatemers in *Xenopus* oocytes to investigate potential electrophysiological differences. ACh elicited robust currents from the D398N mutated concatemer, with amplitudes similar to those of the wild-type $\alpha 5$ concatemer (Fig. 5b). Concentration–response curves for ACh are similar, with an EC_{50} of 1.08 μM and nH of 1.17 for $\alpha 5$ -D398N concatemer (Fig. 5c, Supplementary Table 1). To assess a potential effect of the $\alpha 5$ -D398N mutation on the receptor's desensitization, we analyzed the decaying phase of agonist-evoked responses during prolonged ACh application. We superposed currents traces generated at saturating and subsaturating ACh concentration for the wild-type and D398N concatemers from oocytes coming from the same animal and observed no significant differences (Fig. 5d). After 5 s of a 100 μM ACh treatment, the current remaining corresponds to $61.3 \pm 6.6\%$ of the initial peak of the wild-type $\alpha 5$ and $55.9 \pm 4.4\%$ for the D398N mutant (Fig. 5e). It is noteworthy that, in oocyte, the ACh-gated currents increase intracellular calcium, thereby activating endogenous calcium-activated chloride channels. The measurements performed herein are thus only semi-quantitative, but overall, we could not detect

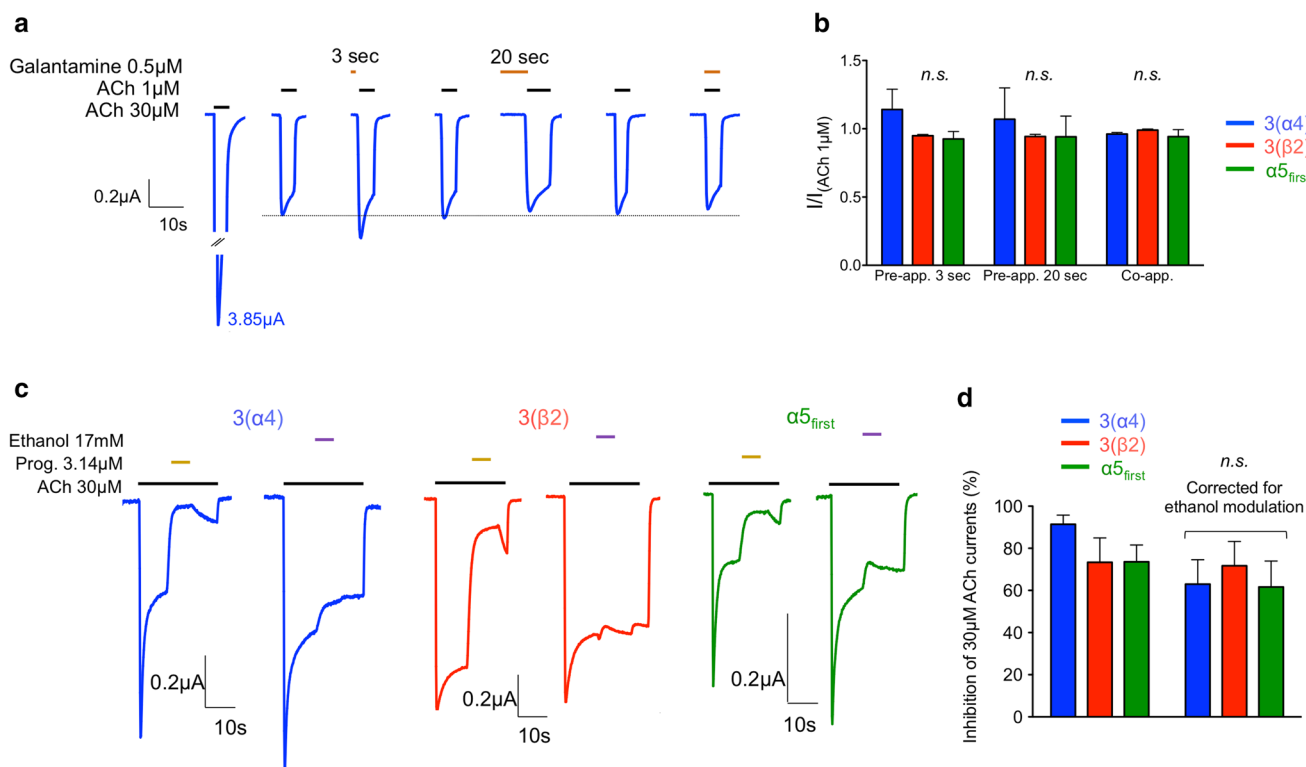


Fig. 4 Galantamine and progesterone fail to selectively modulate $\alpha 5$ -containing concatemers. **a** Sample traces of Galantamine effect on the 3($\alpha 4$) concatemer. Three protocols are displayed for the same cell: a 3-s pre-application, a 20-s pre-application and a co-application of galantamine with a sub-saturating ACh concentrations, showing no effect on the peak current. **b** Normalized peak currents obtained with the three protocols for the three concatemers. The apparent potentiation of 3($\alpha 4$) is not significant as compared with the 3($\beta 2$). Displayed are mean \pm SD with $n \geq 3$. “n.s.” indicates that a one-way ANOVA with a Tukey’s post hoc test was performed and found the values not statistically different from each other. **c** Sample traces of progesterone

inhibition on the three concatemers. For each cell, a control application of 17 mM of Ethanol was performed to account for the ethanol concentration used for progesterone solubilization. **d** Percentage inhibition of 30 μ M ACh-evoked currents by 3.14 mM progesterone. Data on the right are corrected by the ethanol effect for each cell at 17 mM. The corrected values for progesterone inhibition at 3.14 μ M are similar for the three concatemers with $n \geq 3$: $63.0 \pm 12\%$ for 3($\alpha 4$), $71.7 \pm 12\%$ for 3($\beta 2$) and $61.7 \pm 12\%$ for $\alpha 5_{\text{first}}$. “n.s.” indicates that a one-way ANOVA with a Tukey’s post hoc test was performed and found the values not statistically different from each other

any obvious difference between our WT and $\alpha 5$ -D398N concatemers.

Identification of an $\alpha 5$ specific irreversible channel-block reaction

In the course of SCAM (substituted cysteine accessibility method) experiments on the $\alpha 5$ concatemers, we applied the commonly used cysteine-modifying reagent MTSEA. When co-applied with ACh for 20 s, 200 μ M MTSEA inhibited currents of all concatemers (Fig. 6). This inhibition is moderate and reversible upon washing for the 3($\alpha 4$) and the 3($\beta 2$) concatemers, suggesting a pore-blocking effect. However, on the $\alpha 5$ concatemer, this inhibition is stronger and is not reversible upon washing, with still $65 \pm 13\%$ of the current silenced after a 5-min wash (Fig. 6b, it is noteworthy that inhibition is nearly complete (higher than 90%) when using 1 mM MTSEA, Fig. 7). In the $\alpha 5$ sequence, we noticed the

presence of a cysteine residue in the second transmembrane segment (2’ position Cys261) which faces the ion channel lumen (Fig. 6c, d). This cysteine is not present in $\alpha 4$ and $\beta 2$, and is thus a good candidate for $\alpha 5$ -specific covalent reaction with MTSEA. We thus mutated the cysteine to serine ($\alpha 5$ -C261S mutant), which fully abolished the irreversible component of MTSEA inhibition (Fig. 6e), demonstrating that the observed effect is due to the covalent modification of this residue in the channel lumen. In addition, we applied on the $\alpha 5$ concatemer another cysteine-modifying reagent used in SCAM studies, MTSET (Supplementary Fig. 3). We observed that MTSET is also able to irreversibly inhibit the $\alpha 5$ concatemer (40% inhibition after 1 min at 200 μ M), likely through the reaction with the same Cys261.

In conclusion, we identified reagents that irreversibly inhibit human $\alpha 5$ -containing nAChRs while leaving $\alpha 4\beta 2$ receptors unaffected.

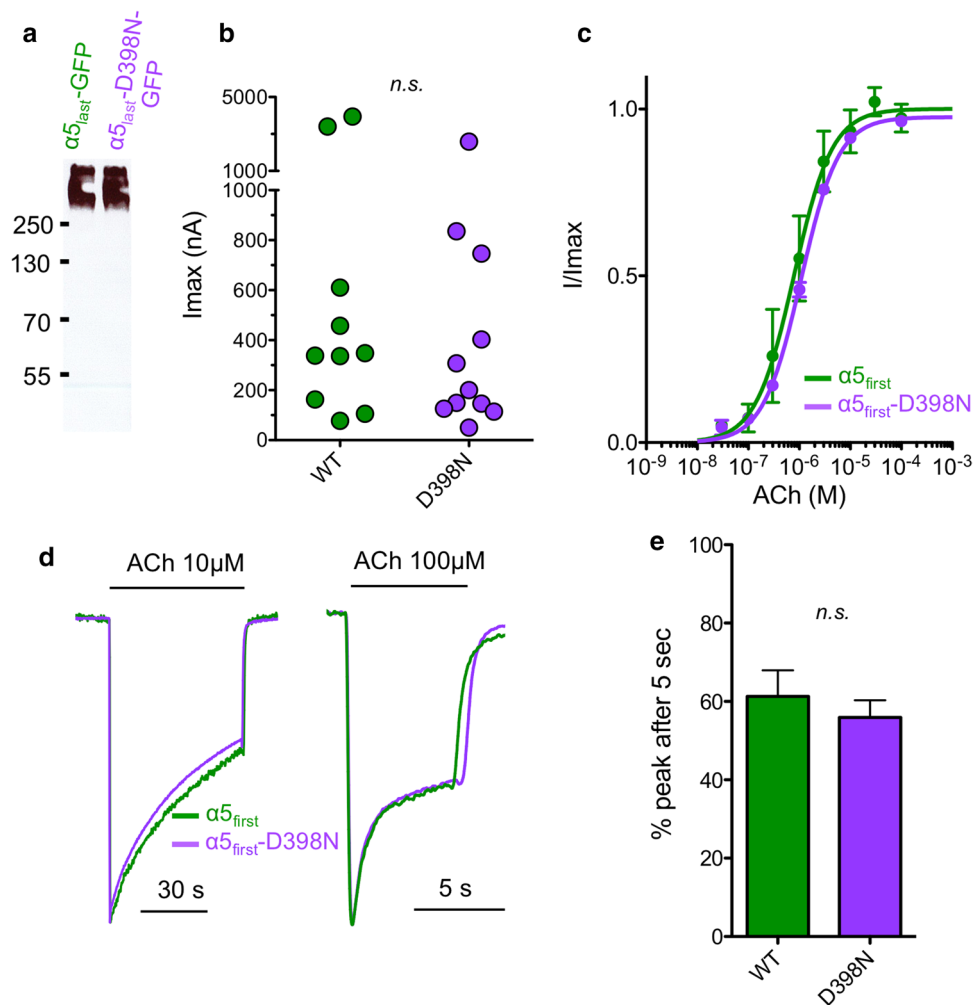


Fig. 5 Apparent lack of functional effects of the $\alpha 5$ -D398N mutation. **a** Anti-GFP western blot of whole cell extracts of HEK cells expressing the WT and D398N $\alpha 5$ concatemers. **b** Scattered dot-plot of maximal currents recorded in oocytes expressing the WT and D398N mutant $\alpha 5$ concatemers. Measurements were performed on injections series where the WT and mutant constructs were injected on the same oocytes batches and recorded the same day. Each dot corresponds to a single cell with $n \geq 10$. “n.s.” indicates that a Student’s t test was performed and found the values not statistically different from each other. **c** ACh concentration–response curves for the $\alpha 5$ concatemers

WT and D398N mutant. Points are mean \pm SD with $n \geq 4$. **d** Sample traces of responses to sub-saturating and saturating ACh concentrations for the WT (green) and D398N (purple) $\alpha 5$ concatemers. Traces were normalized to the peak to facilitate comparison. Oocytes from the same animal were compared. **e** Mean residual current observed after 5 s application of saturating ACh (10 μ M) for the WT and D398N $\alpha 5$ concatemers. Oocytes from the same animal were compared with $n \geq 3$. Displayed are mean \pm SD. “n.s.” indicates that a Student’s t test was performed and found the values not statistically different from each other

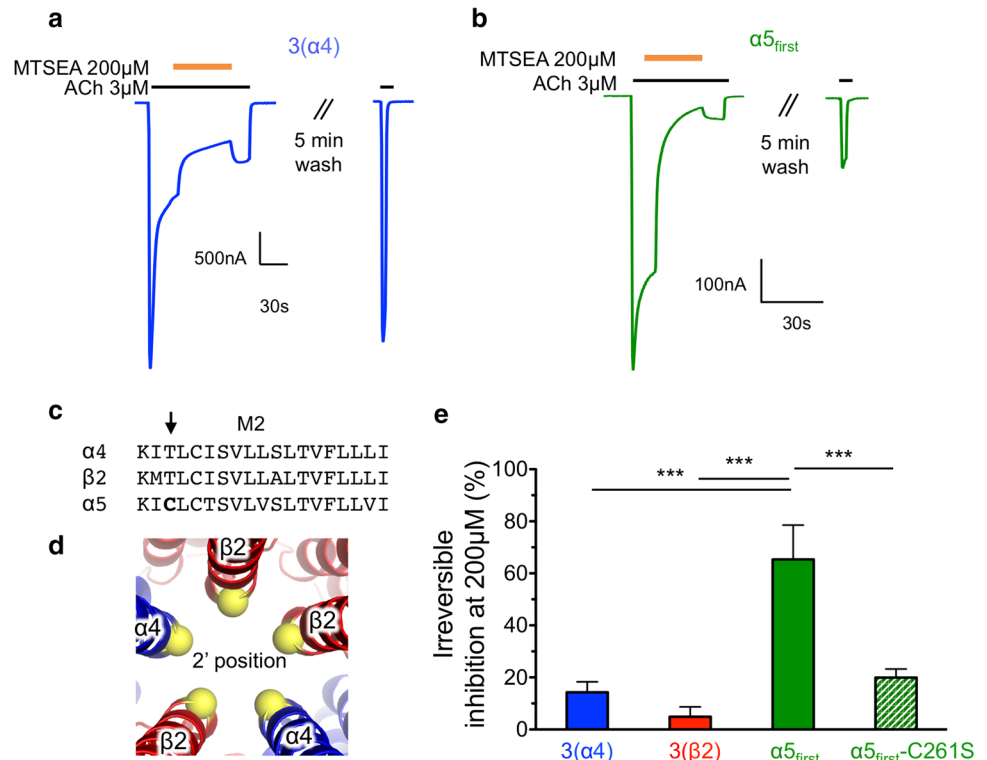
MTSEA as a tool to estimate the $\alpha 5$ content in $\alpha 4\beta 2$ nAChRs

To study $\alpha 4\beta 2\alpha 5$ nAChRs, it is common practice to transfect cells with an excess of $\alpha 5$ -encoding cDNA, a 1:1:10 ratio for $\alpha 4$: $\beta 2$: $\alpha 5$ being in most cases considered as sufficient to generate a majority of $\alpha 5$ -containing receptors population. We challenged this assumption using the specificity of the MTSEA irreversible blockade of $\alpha 5$. We co-injected $\alpha 4$ and $\beta 2$ cDNAs with increasing amounts of $\alpha 5$ cDNAs. We evaluated the irreversible inhibition of ACh-elicited currents by applying 1 mM MTSEA for 30 s in presence of

ACh, followed by a 5-min wash, conditions for which we reach $> 90\%$ inhibition of the $\alpha 5$ concatemer (Fig. 7a, b), incidentally demonstrating that blockade by MTSEA can reach completion by increasing its concentration.

In the absence of $\alpha 5$ (1:1:0), we detect a moderate short-term current inhibition and no irreversible inhibition (Fig. 7c). This is consistent with what we observed for the 3($\alpha 4$) and the 3($\beta 2$) concatemers. At 1:1:1 ratio, we observed no significant irreversible inhibition suggesting that little or no $\alpha 5$ is incorporated. At 1:1:2, half of the cells are not irreversibly inhibited by MTSEA, while the other half display partial irreversible inhibition. At 1:1:6, 1:1:10 and

Fig. 6 Irreversible channel-block of $\alpha 5$ -nAChR by MTSEA. **a, b** Sample trace of the effect of MTSEA (200 μM) on the $3(\alpha 4)$ and $\alpha 5$ concatemers during a 20 s co-application with ACh and after 5 min wash. **c** Sequence alignment of the M2 transmembrane segment for $\alpha 4$, $\beta 2$ and $\alpha 5$. Arrows indicate the cysteine residue in 2' mutated in $\alpha 5$. **d** View from the top of the pore of the $\alpha 4\beta 2$ nAChR X-ray structure visualized using PyMol (Morales-Perez 2018 pdb 5KXI). The α -carbon of each of the 2' residues is depicted as yellow spheres. **e** Mean irreversible inhibition after a 20 s MTSEA (200 μM) + ACh (3 μM) application for the $3(\alpha 4)$, $3(\beta 2)$, $\alpha 5$ and $\alpha 5$ -C261S concatemers. Displayed are mean \pm SD with $n \geq 4$. *** Statistically different from $\alpha 5_{\text{first}}$ (one-way ANOVA with Dunnett's test using $\alpha 5$ as control group, $p < 0.001$)



1:1:12 ratios, the extent of irreversible inhibition progressively increases, but this is associated with a large variability from cell to cell, both between and within oocytes injection batches. At the 1:1:12 ratio, none of the oocytes display the nearly full inhibition of $\alpha 5_{\text{first}}$. At higher ratios, such as 1:1:20, we could not detect currents most of the time, probably because overloading cells with $\alpha 5$ alters the assembly and/or export and/or function of receptors. Overall, even at the highest cDNA ratio of 1:1:12, MTSEA inhibition was highly variable, demonstrating that the population of receptors is still highly heterogeneous with, for most cells, the significant contribution of $\alpha 5$ -less receptors.

Altogether, these results show that for ratios higher than 1:1:6, incorporation of $\alpha 5$ does happen, sometimes in the majority on the pentamers, but is highly variable from cell to cell, and is never complete. This demonstrates that, even in excess of $\alpha 5$ cDNA, injection of loose subunits is not efficient to generate a homogenous population of $\alpha 4\beta 2\alpha 5$ nAChRs.

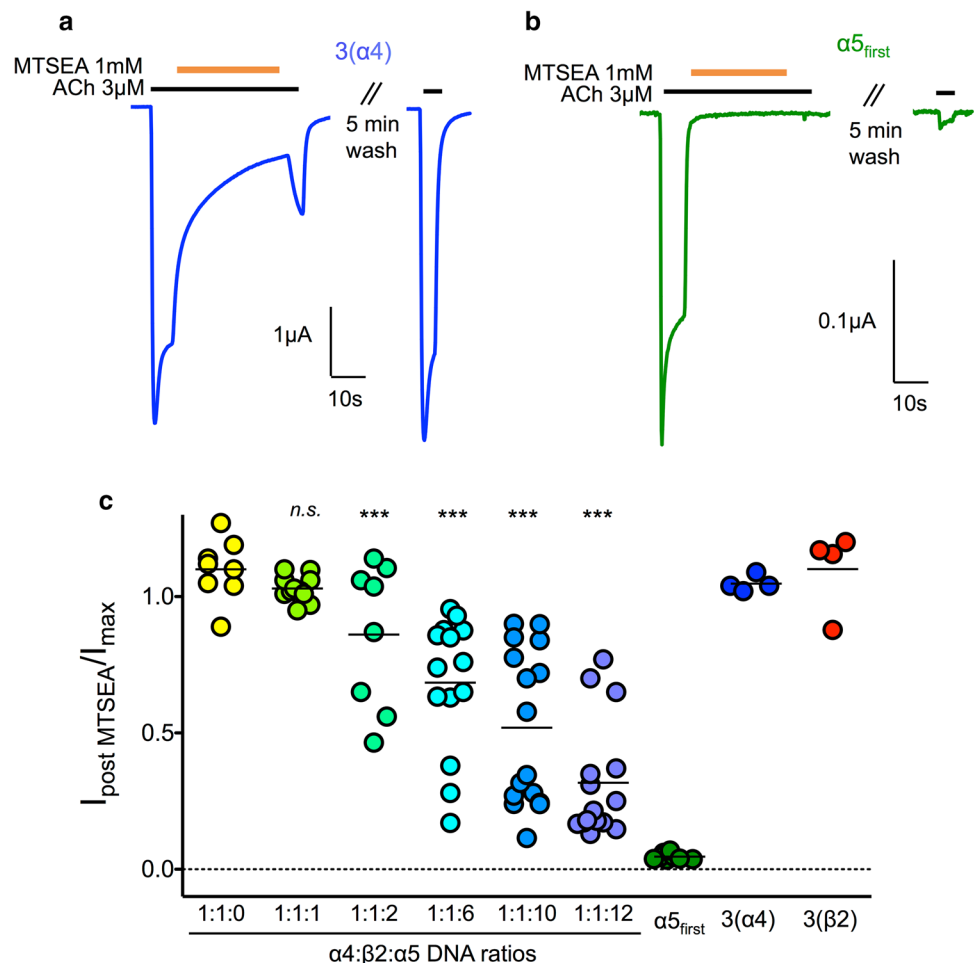
Discussion

Design of concatemers unambiguously and quantitatively expressing $\alpha 5$ -nAChRs

The study of $\alpha 5$ -nAChRs is difficult in recombinant systems that express loose subunits, because the resulting population

is heterogeneous and hardly controlled by the experimenter. Here, we directly illustrate this issue by using our finding that MTSEA irreversibly inhibits only $\alpha 5$ -containing receptor. In our system, even at the highest cDNA 1:1:12 ratio for $\alpha 4:\beta 2:\alpha 5$, we show that oocytes express a heterogeneous population of receptors with the significant contribution of $\alpha 5$ -less assemblies, in a proportion highly variable from cell to cell. Interestingly, in the seminal paper of Ramirez-Latorre et al. [39], the authors used substituted-cysteine accessibility method at several positions in the ion channel of the mouse $\alpha 5$, including the 2' (since mouse $\alpha 5$ carries an endogenous serine at position 2'), to demonstrate the incorporation of $\alpha 5$ into $\alpha 4\beta 2$ nAChRs. Their study, following RNA injection of loose subunits in oocyte, is consistent with ours with a partial (30%) irreversible inhibition of the currents by 1 mM MTSET for the $\alpha 4:\beta 2:\alpha 5(\text{S}2'\text{C})$ at a 1:1:10 ratio, as compared to the (40%) irreversible inhibition by 200 μM MTSET for the $\alpha 5_{\text{first}}$ concatemer. However, our results contrast with those of Marotta et al. [40] which show that, for a 1:1:10 ratio for $\alpha 4:\beta 2:\alpha 5(\text{V}9'\text{S})$ expressed by RNA injection in the oocyte, a nearly homogenous population containing the $\alpha 5(\text{V}9'\text{S})$ subunit, which specifically shows fast-reversible mecamylamine inhibition, is expressed. Since we show here a high variability in $\alpha 5$ incorporation, it is possible that this discrepancy comes from different oocyte sources or RNA versus DNA injection. We also cannot exclude species differences since they used mouse nicotinic subunits for their experiments. Alternatively, it can come

Fig. 7 Evaluation of $\alpha 5$ content in pentamers from loose subunits. **a, b** Sample traces of the effect of MTSEA on the $3(\alpha 4)$ and $\alpha 5$ concatemers during a 30 s 1 mM co-application with ACh and after 5 min wash. **c** Scattered dot-plot presenting the permanent inhibition measured for each cell injected with the indicated DNA ratio and with $n \geq 4$. One-way ANOVA with Dunnett's test using 1:1:0 as control group found those values not different from the 1:1:0 ratio (n.s.) or statistically different with $p < 0.001$ (***)



from the presence of a mutation in the channel pore in the Marotta et al. study (V9'S), since single mutations in the transmembrane domain have been reported to strongly alter subunit assemblies in GABA_A receptors [41].

In the present study, we developed a convenient concatemeric system to force the subunit stoichiometry, which display currents large enough for characterization. We conducted biochemical validation to ensure the integrity of the final protein products after expression, highlighting the absence of any cleavage. Moreover, for the $\alpha 5$ -containing concatemers, we uncovered the irreversible inhibition by MTSEA due to the cysteine in the $\alpha 5$ pore region, thereby fully assigning the electrophysiological currents to $\alpha 5$ -containing receptors. However, we provide evidence that the concatemers assemble according to two orientations, clockwise and anticlockwise, a feature that must be considered when interpreting pharmacological data. In the literature, we found another study describing two concatemeric $\alpha 4\beta 2\alpha 5$ nAChRs. They differ from ours from the linker used and the subunit order [19], which in this case inserts $\alpha 5$ between two $\alpha 4$ s ($\beta 2-\alpha 4-\alpha 5-\alpha 4-\alpha 4/\beta 2$). The resulting constructs displayed low current amplitudes, with maximal

currents around 30 nA, precluding their use for systematic functional and pharmacological investigation.

On the effect of SNP mutant D398N on nAChR signaling

We found no significant effect of the D398N mutation on the concatemeric function, a feature also reported by other groups [11, 38] and which contrasts with its strong effect in the human population, as well as in animal models. We thus speculate that D398N might rather alter other features of the receptor, such as its biosynthesis, cellular trafficking, plasma membrane diffusion and/or internalization processes. In this line, it is noteworthy that the mutation is located in the ICD, which is involved in interaction with cytoplasmic proteins and allosteric regulation by phosphorylation. When looking at the recent cryo-EM structure of the $\alpha 3\beta 4$ nAChR [42] for which part of the ICD is solved, the residues of $\alpha 3$ and $\beta 4$ that are homologous to $\alpha 5$ Asp398 have their side chain accessible to the solvent. This position could thus even be directly involved in interaction with cytoplasmic proteins. Unfortunately, those processes cannot be studied

in recombinant systems, especially *Xenopus* oocytes, as they are far from recapitulating the neuronal conditions.

Our MTSEA assay suggests that $\alpha 5$ incorporation into $\alpha 4\beta 2$ receptors is rather inefficient, since even a large excess of this subunit cDNA does not drive quantitatively the assembly to $\alpha 5$ -containing receptors. It is thus likely that $\alpha 5$ displays a low propensity of assembly with the $\alpha 4$ and $\beta 2$ subunits in the course of maturation within the endoplasmic reticulum, an observation that is in line with the smaller currents recorded on $\alpha 5$ -containing concatemers. This contrasts with the case of $\alpha 3\beta 4$ receptors, where $\alpha 5$ is shown to efficiently integrate into pentamers, and for which pentameric concatemers containing the $\alpha 5$ subunit at the fifth position display stronger currents than $\alpha 5$ -less concatemers [11].

The $\alpha 5$ subunit contribution to ligand binding

Our data support that the principal face of $\alpha 5$ does not contribute to ACh binding, since the $3(\beta 2)$ and $\alpha 5$ -containing concatemers are identical in terms of ACh dose–response curve, which is not altered when the canonical Trp from the $\alpha 5$ principal site is mutated. This idea is fully consistent with a previous work by Marotta et al. [40], where mutation of loops A, B and C of $\alpha 5$ did not alter the ACh dose–response curves as well. In contrast, Jain et al. studied $\alpha 4\beta 2$ concatemeric dimers co-expressed with loose $\alpha 5$ subunits [28]. Their data suggest that ACh does bind to the $\alpha 5$ – $\alpha 4$ and/or $\alpha 5$ – $\beta 2$ interfaces, yet with a lower affinity to that of $\alpha 4$ – $\beta 2$ interface, yielding biphasic ACh dose response curves. Their data also suggest that Saz-A is a partial agonist of $\alpha 5$ -nAChRs yielding an efficacy of approximately 30% relative to Ach [28]. Herein, we did not replicate the Saz-A effect, since applying it on $\alpha 5_{\text{first}}$ elicited robust currents matching ACh-evoked currents ($95.9 \pm 6\%$), pointing to a full agonistic activity. We provisionally propose that such experimental discrepancies might be due to the use of dimeric concatemers, which do not strictly exclude the contribution of nAChRs devoid of $\alpha 5$ subunits, notably the $\alpha 4_3\beta 2_2$ combination, to the whole-cell currents. Indeed, the MTSEA inhibition of our $\alpha 5$ -containing concatemers, which we also observed with MTSET and which we extended to $\alpha 5$ -containing nAChRs assembled from free subunits, hampers the use of MTS compounds for SCAM studies when using human $\alpha 5$ -containing nAChRs. The absence of MTSET inhibition at human $\alpha 5$ -containing nAChRs in the Jain et al. study might thus reflect a substantial contribution of the $\alpha 4_3\beta 2_2$ combination.

Interestingly, we found that sazetidine displays different dose response curves on $\alpha 5$ -containing concatemers as compared to the $3(\beta 2)$. Our data indirectly suggest that it may bind to the $\alpha 4(+)$ – $\alpha 5(-)$ site with a lower affinity than to the classical $\alpha 4(+)$ – $\beta 2(-)$ site. The idea that the $\alpha 4(+)$ – $\alpha 5(-)$ site contributes to ACh binding was already documented

[19], but we suggest here that sazetidine displays significant selectivity for $\alpha 4(+)$ – $\beta 2(-)$ site, opening for further pharmacological investigation.

In light of previous difficulties in studying $\alpha 5$ -containing nAChRs, we also chose to reinvestigate their pharmacology, focusing on ligands that have been proposed to show some selectivity towards these receptors, such as galantamine and progesterone. While the former has no effect on any of our concatemers, the latter appears to be a non-selective inhibitor, modulating $\alpha 4\beta 2$ and $\alpha 4\beta 2\alpha 5$ nAChRs with similar potencies.

In conclusion, our concatemeric designs, which force the incorporation of the $\alpha 5$ subunit, offer a well-characterized platform to screen for allosteric modulators of $\alpha 5$ -containing nAChRs, and decipher their mechanisms of action. These concatemers will also allow for a precise dissection of the gating mechanisms, since they enable to introduce mutations one subunit at a time in the entire pentamer to assess the interactions between subunits, as well as the long-range allosteric communication between distant binding sites, similarly to previous work on GABA_A receptors [23, 43, 44].

Acknowledgements This work was funded by the ERC Grant (No. 788974, Dynacotine), the ANR Grant (No. 17-CE11-0030 Nicofive), the “équipe FRM” (Fondation pour la Recherche Médicale) grant DEQ20140329497, a fellowship from the Fondation ARC to MSP and a European Commission Research Executive Agency individual fellowship to MG (Marie Skłodowska-Curie Action, Individual Fellowship 659371). The authors would like to thank Uwe Maskos, Stéphanie Pons, Morgane Besson, Akos Nemezc and Alexandre Mourrot for critical reading of the manuscript.

Author contributions MSP, MG and P-JC designed the study. MSP, HB, NB and MG performed and analyzed the experiments. MSP, MG and P-JC wrote the manuscript with inputs of all authors.

Compliance with ethical standards

Conflict of interest The authors declare that there are no conflicts of interest.

References

1. Wen L, Jiang K, Yuan W et al (2014) Contribution of variants in CHRNA5/A3/B4 gene cluster on chromosome 15 to tobacco smoking: from genetic association to mechanism. *Mol Neurobiol* 53:472–484. <https://doi.org/10.1124/jpet.107.132977>
2. Salas R, Orr-Urtreger A, Broide RS et al (2003) The nicotinic acetylcholine receptor subunit alpha 5 mediates short-term effects of nicotine in vivo. *Mol Pharmacol* 63:1059–1066. <https://doi.org/10.1124/mol.63.5.1059>
3. Morel C, Fattore L, Pons S et al (2014) Nicotine consumption is regulated by a human polymorphism in dopamine neurons. *Mol Psychiatry* 19:930–936. <https://doi.org/10.1038/mp.2013.158>
4. Fowler CD, Lu Q, Johnson PM et al (2011) Habenular $\alpha 5$ nicotinic receptor subunit signalling controls nicotine intake. *Nature* 471:597–601. <https://doi.org/10.1038/nature09797>

5. Dawson A, Wolstenholme JT, Roni MA et al (2018) Knockout of alpha 5 nicotinic acetylcholine receptors subunit alters ethanol-mediated behavioral effects and reward in mice. *Neuropharmacology* 138:341–348. <https://doi.org/10.1016/j.neuropharm.2018.06.031>
6. Besson M, Guiducci S, Granon S et al (2016) Alterations in alpha5* nicotinic acetylcholine receptors result in midbrain- and hippocampus-dependent behavioural and neural impairments. *Psychopharmacology*. <https://doi.org/10.1007/s00213-016-4362-2>
7. Forget B, Scholze P, Langa F et al (2018) A human polymorphism in CHRNA5 is linked to relapse to nicotine seeking in transgenic rats. *Curr Biol* 28:3244–3253.e7. <https://doi.org/10.1016/j.cub.2018.08.044>
8. Besson M, Forget BXT, Correia C et al (2019) Profound alteration in reward processing due to a human polymorphism in. *Neuropsychopharmacology*. <https://doi.org/10.1038/s41386-019-0462-0>
9. Exley R, McIntosh JM, Marks MJ et al (2012) Striatal 5 nicotinic receptor subunit regulates dopamine transmission in dorsal striatum. *J Neurosci* 32:2352–2356. <https://doi.org/10.1523/JNEUROSCI.4985-11.2012>
10. Grady SR, Salminen O, McIntosh JM et al (2009) Mouse striatal dopamine nerve terminals express $\alpha 4\alpha 5\beta 2$ and two stoichiometric forms of $\alpha 4\beta 2^*$ -nicotinic acetylcholine receptors. *J Mol Neurosci* 40:91–95. <https://doi.org/10.1124/mol.54.6.1124>
11. George AA, Lucero LM, Damaj MI et al (2012) Function of human $\alpha 3\beta 4\alpha 5$ nicotinic acetylcholine receptors is reduced by the $\alpha 5$ (D398N) variant. *J Biol Chem* 287:25151–25162. <https://doi.org/10.1124/mol.63.5.1059>
12. Mazzaferro S, Benallegue N, Carbone A et al (2011) Additional acetylcholine (ACh) binding site at alpha4/alpha4 interface of (alpha4beta2)2alpha4 nicotinic receptor influences agonist sensitivity. *J Biol Chem* 286:31043–31054. <https://doi.org/10.1074/jbc.M111.262014>
13. Ahring PK, Liao VWY, Balle T (2018) Concatenated nicotinic acetylcholine receptors: a gift or a curse? *J Gen Physiol* 150:453–473. <https://doi.org/10.1124/mol.54.6.1124>
14. Groot-Kormelink PJ, Broadbent S, Beato M, Sivilotti LG (2006) Constraining the expression of nicotinic acetylcholine receptors by using pentameric constructs. *Mol Pharmacol* 69:558–563. <https://doi.org/10.1124/mol.105.019356>
15. Carbone A-L, Moroni M, Groot-Kormelink P-J, Bermudez I (2009) Pentameric concatenated (alpha4)(2)(beta2)(3) and (alpha4)(3)(beta2)(2) nicotinic acetylcholine receptors: subunit arrangement determines functional expression. *Br J Pharmacol* 156:970–981. <https://doi.org/10.1111/j.1476-5381.2008.00104.x>
16. Mazzaferro S, Benallegue N, Carbone A et al (2011) Additional acetylcholine (ACh) binding site at $\alpha 4/\alpha 4$ interface of ($\alpha 4\beta 2$) 2 $\alpha 4$ nicotinic receptor influences agonist sensitivity. *J Biol Chem* 286:31043–31054. <https://doi.org/10.1523/JNEUROSCI.0627-09.2009>
17. Benallegue N, Mazzaferro S, Alcaino C, Bermudez I (2013) The additional ACh binding site at the $\alpha 4(+)/\alpha 4(-)$ interface of the ($\alpha 4\beta 2$) 2 $\alpha 4$ nicotinic ACh receptor contributes to desensitization. *Br J Pharmacol* 170:304–316. <https://doi.org/10.1074/jbc.M111.221754>
18. Eaton JB, Lucero LM, Stratton H et al (2013) The unique $\alpha 4(+)/(-)$ $\alpha 4$ agonist binding site in ($\alpha 4$)3($\beta 2$)2 subtype nicotinic acetylcholine receptors permits differential agonist desensitization pharmacology versus the ($\alpha 4$)2($\beta 2$)3 subtype. *J Pharmacol Exp Ther* 348:46–58. <https://doi.org/10.1124/mol.54.6.1124>
19. Jin X, Bermudez I, Steinbach JH (2014) The nicotinic $\alpha 5$ subunit can replace either an acetylcholine-binding or nonbinding subunit in the $\alpha 4\beta 2^*$ neuronal nicotinic receptor. *Mol Pharmacol* 85:11–17. <https://doi.org/10.1124/mol.113.089979>
20. Lucero LM, Weltzin MM, Eaton JB et al (2016) Differential $\alpha 4(+)/(-)\beta 2$ agonist-binding site contributions to $\alpha 4\beta 2$ nicotinic acetylcholine receptor function within and between isoforms. *J Biol Chem* 291:2444–2459. <https://doi.org/10.1124/mol.115.098061>
21. George AA, Bloy A, Miwa JM et al (2016) Isoform-specific mechanisms of $\alpha 3\beta 4^*$ -nicotinic acetylcholine receptor modulation by the prototoxin lynx1. *FASEB J* 31:1398–1420. <https://doi.org/10.1124/mol.115.098061>
22. Mazzaferro S, Bermudez I, Sine SM (2018) Potentiation of a neuronal nicotinic receptor via pseudo-agonist site. *Cell Mol Life Sci*. <https://doi.org/10.1007/s00018-018-2993-7>
23. Gielen MC, Lumb MJ, Smart TG (2012) Benzodiazepines modulate GABAA receptors by regulating the preactivation step after GABA binding. *J Neurosci* 32:5707–5715. <https://doi.org/10.1523/JNEUROSCI.5663-11.2012>
24. Nashmi R, Dickinson ME, McKinney S et al (2003) Assembly of alpha4beta2 nicotinic acetylcholine receptors assessed with functional fluorescently labeled subunits: effects of localization, trafficking, and nicotine-induced upregulation in clonal mammalian cells and in cultured midbrain neurons. *J Neurosci* 23:11554–11567
25. Morales-Perez CL, Noviello CM, Hibbs RE (2016) Manipulation of subunit stoichiometry in heteromeric membrane proteins. *Structure* 24:797–805. <https://doi.org/10.1016/j.str.2016.03.004>
26. Hamouda AK, Deba F, Wang Z-J, Cohen JB (2016) Photolabeling a nicotinic acetylcholine receptor (nAChR) with an ($\alpha 4$) 3 ($\beta 2$) 2nAChR-selective positive allosteric modulator. *Mol Pharmacol* 89:575–584. <https://doi.org/10.1124/mol.54.6.1124>
27. Olsen JA, Ahring PK, Kastrop JS et al (2014) Structural and functional studies of the modulator NS9283 reveal agonist-like mechanism of action at $\alpha 4\beta 2$ nicotinic acetylcholine receptors. *J Biol Chem* 289:24911–24921. <https://doi.org/10.1074/jbc.M114.568097>
28. Jain A, Kuryatov A, Wang J et al (2016) Unorthodox acetylcholine binding sites formed by $\alpha 5$ and $\beta 3$ accessory subunits in $\alpha 4\beta 2^*$ nicotinic acetylcholine receptors. *J Biol Chem* 291:23452–23463. <https://doi.org/10.1016/j.ymeth.2010.01.012>
29. Xiu X, Puskar NL, Shanata JAP et al (2009) Nicotine binding to brain receptors requires a strong cation. *Nature* 458:534–537. <https://doi.org/10.1038/nature07768>
30. Zwart R, Carbone AL, Moroni M et al (2008) Sazetidine-A is a potent and selective agonist at native and recombinant $\alpha 4\beta 2$ nicotinic acetylcholine receptors. *Mol Pharmacol* 73:1838–1843. <https://doi.org/10.1124/mol.54.6.1124>
31. Mazzaferro S, Gasparri F, New K et al (2014) Non-equivalent ligand selectivity of agonist sites in ($\alpha 4\beta 2$) 2 $\alpha 4$ nicotinic acetylcholine receptors. *J Biol Chem* 289:21795–21806. <https://doi.org/10.1113/jphysiol.1989.sp017717>
32. Samochocki M, Höfle A, Fehrenbacher A et al (2003) Galantamine is an allosterically potentiating ligand of neuronal nicotinic but not of muscarinic acetylcholine receptors. *J Pharmacol Exp Ther* 305:1024–1036. <https://doi.org/10.1046/j.1471-4159.2000.0752492.x>
33. Kuryatov A, Onksen J, Lindstrom J (2008) Roles of accessory subunits in $\alpha 4\beta 2^*$ nicotinic receptors. *Mol Pharmacol* 74:132–143. <https://doi.org/10.1074/jbc.273.44.28721>
34. Kowal NM, Ahring PK, Liao VWY et al (2017) Galantamine is not a positive allosteric modulator of human $\alpha 4\beta 2$ or $\alpha 7$ nicotinic acetylcholine receptors. *Br J Pharmacol* 175:2911–2925. <https://doi.org/10.1124/mol.54.6.1124>
35. Valera S, Ballivet M, Bertrand D (1992) Progesterone modulates a neuronal nicotinic acetylcholine receptor. *Proc Natl Acad Sci USA* 89:9949–9953. <https://doi.org/10.1073/pnas.89.20.9949>
36. Kuryatov A, Berrettini W, Lindstrom J (2011) Acetylcholine receptor (AChR) $\alpha 5$ subunit variant associated with risk for nicotine dependence and lung cancer reduces ($\alpha 4\beta 2$)₂ $\alpha 5$ AChR

- function. *Mol Pharmacol* 79:119–125. <https://doi.org/10.1124/mol.110.066357>
37. Tammimäki A, Herder P, Li P et al (2012) Impact of human D398N single nucleotide polymorphism on intracellular calcium response mediated by $\alpha 3\beta 4\alpha 5$ nicotinic acetylcholine receptors. *Neuropharmacology* 63:1002–1011. <https://doi.org/10.1016/j.neuropharm.2012.07.022>
 38. Li P, McCollum M, Bracamontes J et al (2011) Functional characterization of the $\alpha 5$ (Asn398) variant associated with risk for nicotine dependence in the $\alpha 3\beta 4\alpha 5$ nicotinic receptor. *Mol Pharmacol* 80:818–827. <https://doi.org/10.1124/mol.111.073841>
 39. Ramirez-Latorre J, Yu CR, Qu X et al (1996) Functional contributions of alpha5 subunit to neuronal acetylcholine receptor channels. *Nature* 380:347–351. <https://doi.org/10.1038/380347a0>
 40. Marotta CB, Dilworth CN, Lester HA, Dougherty DA (2014) Neuropharmacology. *Neuropharmacology* 77:342–349. <https://doi.org/10.1016/j.neuropharm.2013.09.028>
 41. Hannan S, Smart TG (2018) Cell surface expression of homomeric GABA A receptors depends on single residues in subunit transmembrane domains. *J Biol Chem* 293:13427–13439. <https://doi.org/10.1002/prot.22488>
 42. Gharpure A, Teng J, Zhuang Y et al (2019) Agonist selectivity and ion permeation in the $\alpha 3\beta 4$ ganglionic nicotinic receptor. *Neuron* 104:501–511.e6. <https://doi.org/10.1016/j.neuron.2019.07.030>
 43. Szabo A, Nourmahad A, Halpin E, Forman SA (2019) Monod–Wyman–Changeux allosteric shift analysis in mutant $\alpha 1 \beta 3 \gamma 2L$ GABA A receptors indicates selectivity and crosstalk among intersubunit transmembrane anesthetic sites. *Mol Pharmacol* 95:408–417. <https://doi.org/10.1038/81800>
 44. Absalom NL, Ahring PK, Liao VW et al (2019) Functional genomics of epilepsy-associated mutations in the GABA A receptor subunits reveal that one mutation impairs function and two are catastrophic. *J Biol Chem* 294:6157–6171. <https://doi.org/10.1371/journal.pone.0141359>

Publisher's Note Springer Nature remains neutral with regard to jurisdictional claims in published maps and institutional affiliations.